

PULSE, A Waveform Model for River Isotopic and Chemical Time-series Data

Mohamed Fahmy Hussein (✉ profdrfahmy@cu.edu.eg)

Cairo University, Egypt <https://orcid.org/0000-0003-0891-212X>

Kamal Zouari

École Nationale d'Ingénieurs de Sfax, ENIS, Tunisie

Mohamed Anter

National Water Research Center, Egypt

Mariam Nosser

Cairo University, Egypt

Research Article

Keywords: Isotope Hydrology, Waveform, Sinusoidal model, River Water EC Oscillation

Posted Date: September 10th, 2020

DOI: <https://doi.org/10.21203/rs.3.rs-56323/v4>

License: © ⓘ This work is licensed under a Creative Commons Attribution 4.0 International License.

[Read Full License](#)

PULSE, A Waveform Model for River Isotopic and Chemical Time-series Data

Mohamed Fahmy Hussein¹, Kamal Zouari², Mohamed Anter³, and Mariam Nosser⁴

¹ profdrfahmy@cu.edu.eg, ² kamel.zouari@enis.tn, ³ mohamed_anter@nwr.gov.eg,

⁴ mariamnosser93@gmail.com

¹ <https://orcid.org/0000-0003-0891-212X>

¹ Corresponding author

^{1,4} Cairo University, Egypt, ² École Nationale d'Ingénieurs de Sfax, ENIS, Tunisie,

³ National Water Research Center, Egypt.

Abstract

The isotopic compositions, electrical conductivity (EC), and ion concentrations frequently change with time in river water worldwide, on various time scales. Periodicity is also known for precipitation and other aqueous inputs. The time-series follow up of such temporal variations is usually to proceed by many hydrologists. The major purpose is to gain a thorough understanding of the underlying phenomena and to plot the data accurately. However, there is no appropriate formula for the graphic illustration and mathematical expression of such time-dependent fluctuations other than the complicated Fourier Series. Also, the use of the standard trigonometric sinusoidal function is not possible due to constraining the output of the values between +1 and -1. In contrast, the isotopic compositions require negative and positive values on the y-axis corresponding to time on the -x-axis, while the hydrochemical concentrations only admit positive values. These constraints are entirely void in the flexible waveform PULSE model proposed in this work. In this model, we introduce a modified sinusoidal formula that has the exciting capability of freely controlling the graphic waveform, in a highly accommodating way, for plotting the time-series isotopic and hydrochemical pulses in conformity with field observations. Three main parameters, and two optional secondary parameters, are to use in our model, open to modification. The model is to use in Excel[®], whose SOLVER built-in macro may give the approximate values for the main parameters. Such values are then to improve to get the waveform best visual fit manually. We applied PULSE on EC, Cl, and $\delta^{18}\text{O}$ values for Nile water, Cairo, and progressively improved the parameters' values as new data was to obtain. The sexagesimal angles are to handle for plotting the sampling dates on the x-axis. The angle that corresponds to one day = $360^\circ/365.24 \text{ day}^{-1} = 0.9856^\circ \text{ day}^{-1} = 0.0172 \text{ rad day}^{-1}$. The standard Excel[®] time and date-models are also to use to assign the time-series sampling dates. The two optional parameters, β and γ , are to use only to damp or expand a decayed or stretched future pulses; otherwise, the values of those secondary parameters should be zero. The far parent of our fundamental PULSE formula is a three-parameter flickering medical equation (*Sinusoidal Amplitude-modulated Flicker Model*) used in the optical-fitness experiments run for testing the human vision adaptation to light luminance, using the appropriate electrophysiological devices. PULSE stands alone in its hydrological category. This model offers a unique quantitative definition for the isotopic and hydrochemical pulses in successive waveforms, with adjustable values for its parameters, in response to the involved variable and the sampling dates. Measurements on Nile water, using daily river water sampling for several years, were to carry out. PULSE revealed its practical merits for an extensive Nile water data set. Such data are for $\delta^{18}\text{O}/\text{V-SMOW} \text{ ‰}$, EC dS m^{-1} , and Cl mg l^{-1} , PULSE works fine for such a riverine system. This application included a rare event of exceptional runoff suddenly imposed on Cairo Nile water composition by a scarce flash thunderstorm, where unusual waveforms were to assign to the isotopic and chemical trails of such abnormal runoff in the Sahara. Such a rare event was to use to get a backward look to the paleo-hydrology of the Nile water composition in Egypt.

KEYWORDS Isotope Hydrology; Waveform; Sinusoidal model; River Water EC Oscillation.

Introduction

The research worker in fluvial hydrology usually obtains qualitative and quantitative observations in both space and time. Such variables are to measure in the field and the laboratory. Finding a suitable mathematical data-presentation method occupies a vital role in the interpretation of the recorded observations in both the community-reports and academic publications. The quantitative treatment of the riverine hydrological system makes data much more representative of the concerned phenomena, hidden under the mass of evidence, than the qualitative methods. The time-series record of the hydrochemical and isotopic variables in fluvial hydrology deals with data-collection, at a specific location, data analysis, and graphical visualization within the selected laps of time, to get a valid interpretation of the involved phenomena. The long-term record of dynamic changes in river water chemistry and isotopic composition could be challenging since this effort needs enough resources and personnel. However, the hard part of the time-series study is to render the collected observations readable and their interpretation meaningful albeit the presence of multiple contributions to water-composition change in the river stem with time (runoff, baseflow, urban zone impact, human intervention to store water in artificial lakes in front of dams to combat high and low floods, pollution of agricultural and industrial origins, and other anthropogenic aqueous inputs). The long-term record of the hydrochemical river-water variables may show several ups and downs in quasi-regular patterns along the hydrological year. It is crucial to find an appropriate mathematical formula that can illustrate the multiple temporal variations that may include rare anomalous events.

This work presents a new waveform to express the temporal changes in river water chemical composition, namely the solute load, and the isotopic ratio (e.g., $\delta^{18}\text{O}$). The approach for finding a flexible waveform formula may give trails to specific trigonometric or polynomial functions; however, the shouting-out of the plausible range and the impossible usage of negative values in some of these functions blocks its applicability to river hydrology. The suitable waveform model must have a small number of parameters and should be open to the introduction of more parameters as needed in specific cases of application to change the oscillation-pace as well as the amplitude, slope, and trend. The most important feature of the required waveform model is to flexibly accept negative and positive values on the y-axis with no restriction in its mathematical structure. An application for the Cairo Nile water EC waveform is to discover in this work using the introduced PULSE model, while the obtained $\delta^{18}\text{O}$ and Cl waveforms appear in another work.

Materials and Methods

River Nile water samples were to collect daily, by mid-day, at the middle of the Nile course, one kilometer south of Cairo University, starting late October 2016 and up to the present day. Sampling will be further going for one extra year span. Each water sample was to collect in two fractions, the first to fill a half-liter clean plastic bottle, while the second is a 13.80 ml fraction in a small glass vial, both filled to the top and carefully plugged. Water in the small vials was to reserve for the isotopic measurements, $\delta^{18}\text{O}$ and $\delta^2\text{H}$ (not shown in this work), whereas the half-liter bottles were to use in EC and pH measurements and the rest of their water volumes were to conserve in the refrigerator for later chemical analysis. The electrical conductivity, EC, and the pH readings were immediately obtained by Hanna™ Instruments double-electrode, whose reading was to automatically correct to 25°C. The chloride ion concentrations were also to measure using Hanna™ specific-ion electrode. Such immediate measurements and posterior chemical analyses were to run using the standard atomic absorption and titration methods at Cairo University and the Central Laboratory of the Ministry of Water Resources, Kanater Khayria Research Kernel, 20 km northwest of Cairo.

The determinations of the isotopic ratios, $\delta^{18}\text{O}$ and $\delta^2\text{H}$, in the Nile water samples were to run abroad, after international shipment to Tunisia. Such determinations were to obtain using laser quenching (ABB LGR-ICOS Los Gatos Research Tunable-Diode Laser Analyzer) known as (Off-Axis Integrated Cavity Output Spectroscopy, OA-ICOS) at the Radio-Analyses et Environnement, LRAE,

École Nationale d'Ingénieurs, ENIS), Sfax, Tunisia, in duplicates. In parallel with the daily in situ fresh Nile water sampling and measurements, lab experiments were to run (in the period April 18 to September 17, 2017), at Cairo University, to follow the changes in the EC and isotopic compositions ($\delta^{18}\text{O}$ and $\delta^2\text{H}$) of Nile water stocks stored in multiple evaporation pans, first in the lab, and then in a class-A pan in the field, at the Water Resources Research Station, Zankaloune, Zagazeig, 100 Km northeast of Cairo, in Winter and Summertime of the year 2020. The chemical and isotopic changes in Nile water during non-steady-state evaporation experiments can give a further interpretation of the results of the daily Nile water samples collected, studied, and plotted in several years at Cairo, where the river water is only subject to steady-state evaporation. However, the detailed findings of the non-steady-state evaporation experiments are to publish elsewhere.

Fundamental Formula for PULSE Waveform Model

The PULSE waveform model (Eq 1.A and B, Eq. 2, and Fig 1) was to develop on Excel™, where the built-in SOLVER macro was to run to obtain the values of model parameters by the minimization of the sum of squares of deviation. The divergence is between the daily measured EC and the calculated $f(t)$, both in dS m^{-1} (or between the observed and predicted $\delta^{18}\text{O}/\text{V-SMOW} \%$, or the same again but for Cl ion concentrations). The computed $f(t)$ was initially for the luminance, in the medical formula, KELLY, 1972, that we have initially adopted to develop our PULSE carrier-signal model. Continuous posterior adjustments of the obtained values for model parameters were to manually carry out to get visual curve best fit as more EC values, Cl concentrations, and $\delta^{18}\text{O}$ data-point ratios were to add to the spreadsheet progressively. The PULSE model periodic-waveform is to use to generate the frequency response useful in the interpretation of the time-dependent hydrochemistry and isotope hydrology data sets. The model calculates the signal value, $f(t)$ corresponding to each data-point, using either three parameters (L, m, and T) or five parameters (when the optional parameter β is to include, with its start factor γ as internal modifier) in the periodic-time-versions (Eq 1.A and B) and the frequency-version (Eq 2). The start factor, γ , is not shown in the equations since it is an internal modifier of the parameter β .

$$f(t) = L * [1 + (m - (m\beta/100)) * (\sin(\theta/(T * 0.985547362)))] \dots \dots \dots (1.A)$$

$$f(t) = L + (L * (m - (m\beta/100)) * (\sin(\theta/(T * 0.985547362)))) \dots \dots \dots (1.B)$$

$$f(t) = L + (L * (m - (m\beta/100)) * (\sin(\theta * (fr * (1/0.985647362)))) \dots \dots \dots (2)$$

with

- L average of the pulse, mg l^{-1} , or dS m^{-1} , for ionic concentrations and EC, respectively, or in per mil for isotopes (e.g., $\delta^{18}\text{O}$). The L value is constant for the record, and its unit is as for $f(t)$,
- m modulation ratio (called contrast) = (the maximum minus the minimum) divided by (the maximum plus the minimum), where the maximum and minimum values are for the signal value, $f(t)$, on the y-axis, $0 < m < 1$, in response to the angular frequency of the carrier input ω , on the x-axis. However, m in the medical formula is the ratio of direct current, dc, to alternating current, ac, for the vision-test devices used in electrophysiological measurements, dimensionless. The product mL is the amplitude that shows the climax of the peak above the average value,
- T periodic time = $\theta/\omega = 2\pi/\omega$, year,
- t time, days, expressed in angle θ , rad, in our formula (seconds in the medical formula),
- θ the angle used to express the date of the concerned day, = ωt , and $2\pi = \omega T$, rad,
- ω carrier input angular frequency, $\theta/t = 2\pi/T = 2\pi fr$, rad y^{-1} (rad sec^{-1} in the medical formula),
- fr carrier frequency, y^{-1} (Hz in the medical formula),
- β damping parameter used to modify the value of m partially. The β parameter is to further adjust the value of m via the start factor modifier, γ , where β and γ values are to control manually down the column used in computing $f(t)$ in the spreadsheet, dimensionless,
- γ start factor used in modifying the value of the parameter β , dimensionless.

The roles of the primary parameters are

- 1- Amplitude modulation (modification) ratio. This parameter controls the peak amplitude, mL, and the peak-to-trough amplitude, 2mL, of the modulating signal (here the transmitted EC information) to perceive on the y-axis. The user may manually increase (modulate) or decrease (demodulate) the strength of the EC signal to force the waveform to fit the observed EC data-points tightly, after using its first value predicted by SOLVER.
- 2- Average of the modulating signal. This parameter shifts the vertical position of the whole modulating signal (here the EC information) relative to the y-axis. The value of the average parameter is first to insert freely and then to calculate as half of the two y-axis readings for the peak and trough of the waveform when the diagram gets populated with data-points
- 3- Periodic Time of the carrier signal. Changing the T value will result in changing the carrier frequency, $fr = 1/T$, that expresses the number of pulses of the waveform per year (to perceive on the x-axis). The T parameter controls the horizontal locus and pace, of the entire waveform pulses, on any diagram showing the relationship between the concerned variable and date. The value of the carrier frequency, fr , relates to the angular frequency of carrier input ω , by double pi.

Results and Discussion

The collected data set (late 2016 to early 2020) was to construct using daily EC measurements in dS m^{-1} , Cl in ppm, and $\delta^{18}\text{O}/\text{V-SMOW } \%$ as the modulating signals. The study will be further going on for one more year. Only EC data is to use in this work for waveform best fit. The introduced waveform model is highly successful in the visualization of such hydrochemical data. The values of model parameters are consistent with the current river water-management that started to take place by the complete control of Nile flow downstream to Cairo and then to the Delta by the High Dam, at Aswan, for about 50 years. However, the PULSE model is to further test for similar data to collect at Khartoum, Sudan, south of Lake Nasser, north of Aswan, and at the northern river mouths at the coast of the Mediterranean. Other hydrochemical variables are also to plot using this waveform model to check its applicability in the visualization of the conservative vs. the non-conservative chemical variables. A personal record is to compare with historical monthly data sets for TDS in ppm to check the validity of the sampling interval (one sample per day). Significant improvement on the Nile EC waveform is to expect when automatic optical devices become available to get hourly EC measurements at several locations in the long river course.

The PULSE waveform showed powerful when the data set is not fragmented, and when the sampling rate is adequate (i.e., daily vs. monthly). Interestingly, the comparison of recent data with the historical archive revealed how much the Nile trunk south of Cairo has progressively become the ultimate trap of solutes contained in the backflow draining out from the cultivated lands in Upper Egypt during the last five decades as a 150 to 250% increase in the solute loads is strikingly to observe.

Most of the increase in river-water solute load is due to leaching, baseflow, and dissolution, whereas the contribution of evaporation (despite its significance in the river water mass-balance) shows much less contribution to solute load increase in the Nile water.

The later evidence was to obtain *via* the EC- $\delta^{18}\text{O}$ charts (not shown). Electrical conductivity is the easiest way to get an idea about the river solute load; however, EC is not conservative, while chloride is a conservative ion. In contrast, the isotope ratio, $\delta^{18}\text{O}$, is an excellent tracer of water provenance, mixing, and evaporation. Accordingly, the waveform is also to test against the chronological data sets for the chloride ion concentrations.

The critical finding for the Cairo Nile EC waveform is the comparison of the obtained periodic time with the river water residence-time in the sizeable artificial lake Nasser reservoir in the south of Egypt. Cairo Nile EC waveform has produced a periodic time of about 1.04 years, while the mass-

balance of Lake Nasser is showing a couple of years residence-time. The obtained T value for Cairo Nile affirms that the Lake reservoir can only ensure water supply downstream in Egypt for about one extra year if the inflow to the lake is to become absent. Such a limited hydro-margin reserve is too fragile. This point, once again, reflects the utility of the introduced model as a powerful tool. Hopefully, with this type of waveform, one may solve a complex issue like the residence time of water in a large river basin with simple means. Besides, the obtained periodic time, T, of about one year for Cairo Nile water means a short transport time of the river water northward to the Capital.

Moreover, the rare event of a massive thunderstorm in Upper Egypt, late October 2016, was detected in the River Nile chemistry at Cairo, and a small waveform was to construct for this anomalous event. Such a rare rainfall storm revealed the isotopic composition, $\delta^{18}\text{O}$, of the paleo-water masses that were to receive in the Nile basin in Egypt, in the early and middle Holocene, via comparison with the isotopic compositions of groundwater stored in the Wadi Natron aquifer to the southwest of the Nile Delta. This assessment is to appear in another work.

Besides, the daily ups and downs of the observed EC-values, above and below the waveform fitted for Nile water EC during the work period (Oct 2016 – Jan 2020), show irregular micro-mass fronts (river water surges) flowing in Upper Egypt Nile trunk northward to the Capital.

The current river system, of the downstream Nile, as expressed by the obtained EC waveform, is showing TDS trough, Fig. 1, in Summer (June-July-August), and two peaks in Winter (e.g., the transition of Winter 2016/17 and Winter 2017/18). The present-day river solute regime has progressively established during the last few decades, after the construction of the High Dam, 10 km to the south of Aswan city in the south of Egypt.

Comparison with TDS historical data, Fig 2, namely for the monthly-data of the years 1954, 1964, 1973, and 1979 (Khalil and Faaiyiz Saaleyb Hannna, 1984) reveals that the currently ongoing river water chemical composition has developed to the worse in terms of the river turned out to become a drain of its floodplain in Upper Egypt. During the historical floods, WEB 1 and WEB 2, that dominated the Nile flow in Egypt (before the partial cease of 1964 flood, and then the total flood halt by 1970), the lowest TDS values were appearing by the period of the annual flood peak, by late Summer time and early Autumn (i.e., in the three months of August-September-October). However, there were no strong TDS troughs in the two years 1954 and 1964.

Higher TDS values were prevailing in the river water during the rest of each year (previously called the "drought" stage) under the natural system that dominated Nile water flow in Egypt before the construction of the Aswan High Dam (called the "old water regime") during the 9-month river low-stage, as contrary to the case during the 3-months of the annual flood season, Fig 2.

The year 1964 was unfortunate for the TDS-historical data record since it has seen the first "partial-closure" of the River Nile trunk in Egypt (for the deviation of the river-course at a site about 10 km to the south of Aswan city, to allow the construction of the High Dam in the river main channel). This "partial river closure" in the year 1964 had resulted in a temporary TDS increase at Cairo, within about one month, since the river flow was slow before the arrival, in the late months of that year, of the next flood (that was also partially stopped for allowing the progress of the High Dam construction.)

The historical archive of the two particular years 1973 and 1979, Fig 2, shows that Cairo Nile water TDS-trough has already started to turn out to appear earlier, i.e., during June and July (instead of August, September, and October, under the natural system that dominated the river water flow before the High Dam construction). This significant time-shift to the early appearance of the TDS-trough. Such a shift is to observe up to the present-day. This precocious TDS trough is due to the release of higher discharge (from the water stock in Lake Nasser) in Spring and Summertime. This massive water discharge downstream in Spring and early Summertime is to comply with the high Spring and Summer cultivation water-demand (corresponding to the "third crop" cultivation policy, that started to apply in the country shortly after the completion of the High Dam construction to partially fulfill the food demand in Egypt). Such water management and cultivation policies are to shortly revise to efficiently meet with the acute current Nile crisis and climate change as Egypt has no freshwater resources other than the limited River Nile water in the dry Sahara.

Conclusion

The introduction of an easy to use waveform model was needed to freely visualize the frequent temporal changes in river water chemistry and its isotopic composition without the limitations imposed on the oversimplified sinusoidal functions or the extra-complex Fourier series. In this respect, the three- to five-parameter PULSE model, once installed in a spreadsheet, reveals the principal behavior of any fluvial system. The involved calculations imposed the substitution of the 365.24218 days of the calendar year by 360° sexagesimal, and by the corresponding radian angles. The model is also to use for the characterization of precipitation and even for predicting hidden paleo-groundwater recharge events in the river floodplain when archive $\delta^{18}\text{O}$ data is available. Nonetheless, the full application of such a new formula further needs more verification of its utility in following-up the non-conservative solutes vs. the conservative solutes and other isotopes in the stream water. Daily sampling is to recommend for getting a good outcome of such a waveform model. The best achievement for the EC waveform, however, will be the result of using automated EC measurements on the hourly time scale, using adequate optical devices. A copy of the Excel[®] workspace is to obtain from the author upon request.

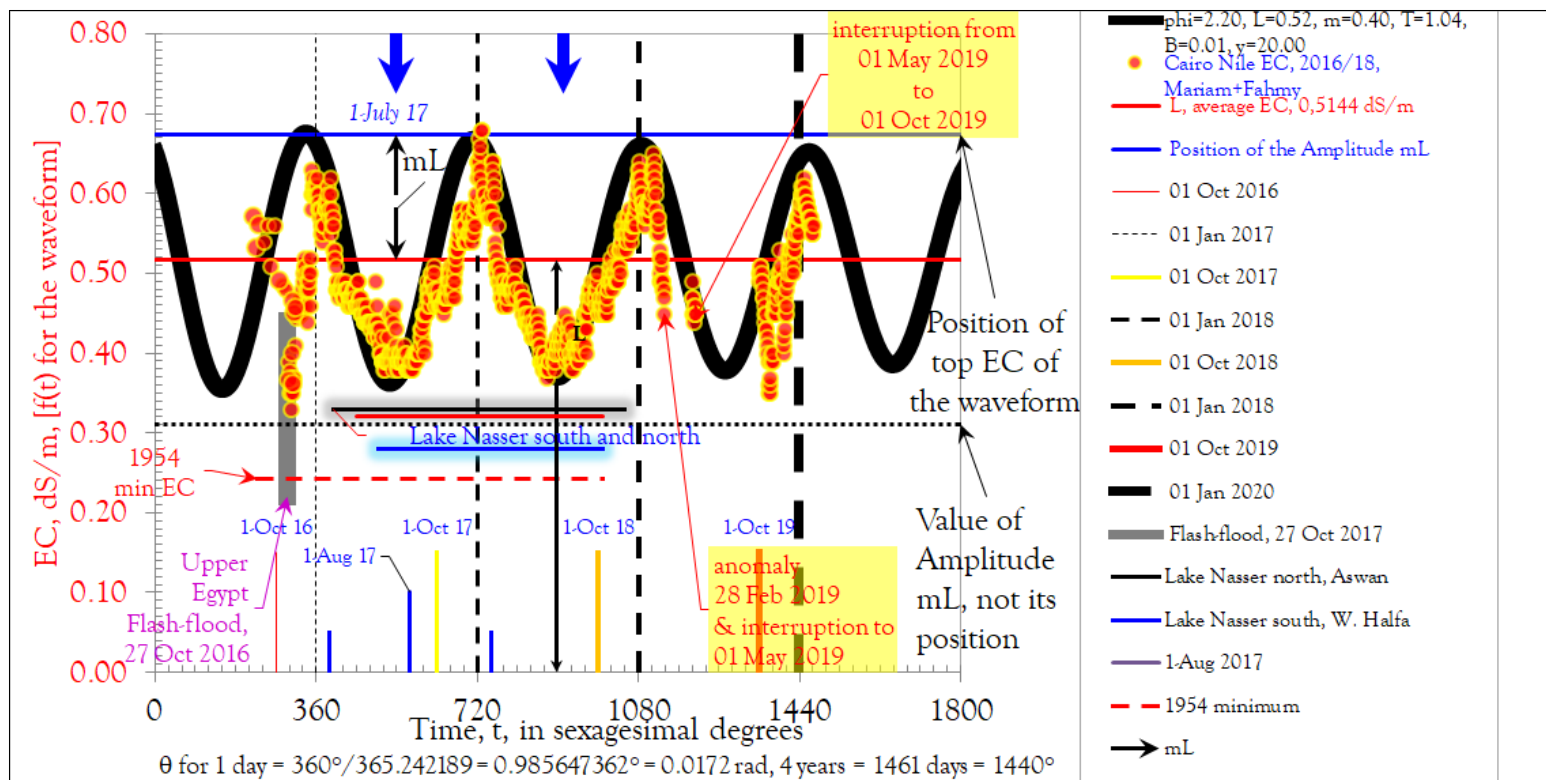


Figure 1 The waveform model fitted to the EC, dS m^{-1} , values for Cairo Nile water. The obtained waveform was to improve via introducing more measurements over four years.

$$f(t) = L * [1 + (m - (m\beta/100)) * (\sin(\theta/(T * 0.985547362)))] \dots \dots \dots (1.A)$$

$$f(t) = 0.5712 * [1 + (0,40 - (0.40 * 0.01/100)) * (\sin(\theta/(1.0416 * 0.985547362)))] \dots$$

with $\gamma = 20.00$

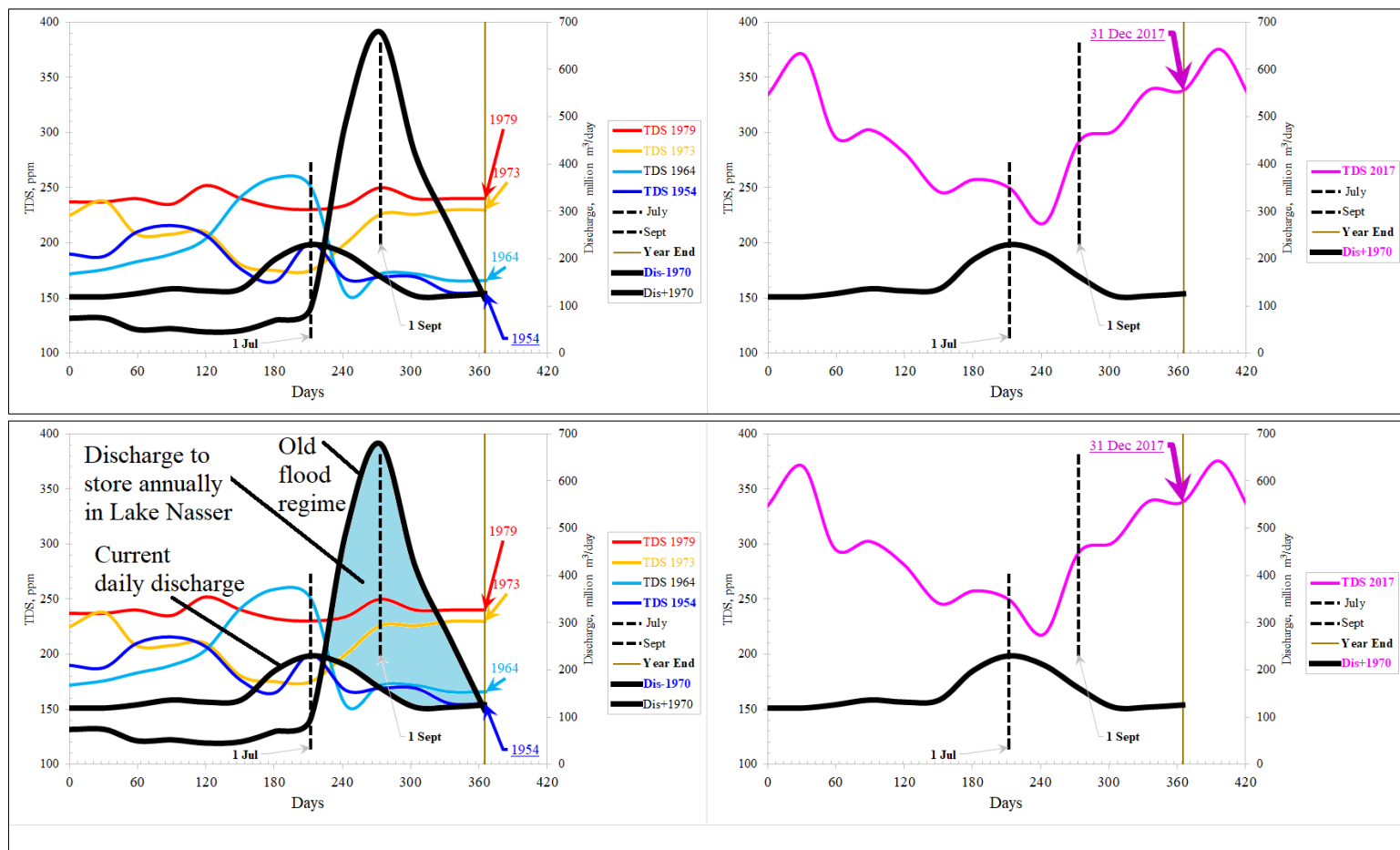


Figure 2 Diagrams showing the old (left) and the current (right) NILE discharge and TDS values at Cairo.

Acknowledgment

We thank Miss Mariam Nossier for Nile water sampling and lab measurements, at Cairo University, Egypt. Special thanks are friendly extended to the Sfax University Isotope Laboratory Staff Members, Tunisia, for good interest in carrying out the ¹⁸O and ²H isotope measurements on our water samples.

Conflict of interest

We have no conflict of interest to declare.

References

- Khalil J B and Faaiyiz Saaleyb Hannna, 1984. Changes in the Quality of Nile Water in Egypt During the Twenty-Five Years, 1954-1979. *Irrig Sci* (1984) 5:1-13. Springer-Verlag.
- KELLY, D H, 1972. Flicker, Ch. 11 (Pages 273-302), in *Visual Psychophysics*, Jameson, Dorothea, Hurvich, Leo. M. (Eds.), in *Autrum, H. (Eds): Handbook of Sensory Physiology, Vol 7, 2012*, reprint of the original 1st ed. 1972. Springer-Verlag. ISBN13 9783642886607. 812 pages.
- <https://www.springer.com/gp/book/9783642886607>
- <https://www.bookdepository.com/Visual-Psychophysics-Dorothea-Jameson/9783642886607>
- <https://books.google.com/eg/books?id=JcF7CAAAQBAJ&pg=PA276&lpg=PA276&dq=can+we+generate+non-negative+values+by+sin?&source=bl&ots=MLJZdY2hd1&sig=wndPc8AKRSIi1rN8Ktf9y8WxOQ8&hl=en&sa=X&ved=0ahUKEwj84buvw9rLAhUHShQKHUKJC-cQ6AEIITAB#v=onepage&q&f=false>
- WEB 1. http://www.geotimes.org/apr05/feature_NileFloods.html
- WEB 2. <https://www.scribd.com/document/251548900/Climate-Change-Nile-Floods-and-Riparia>

Figures

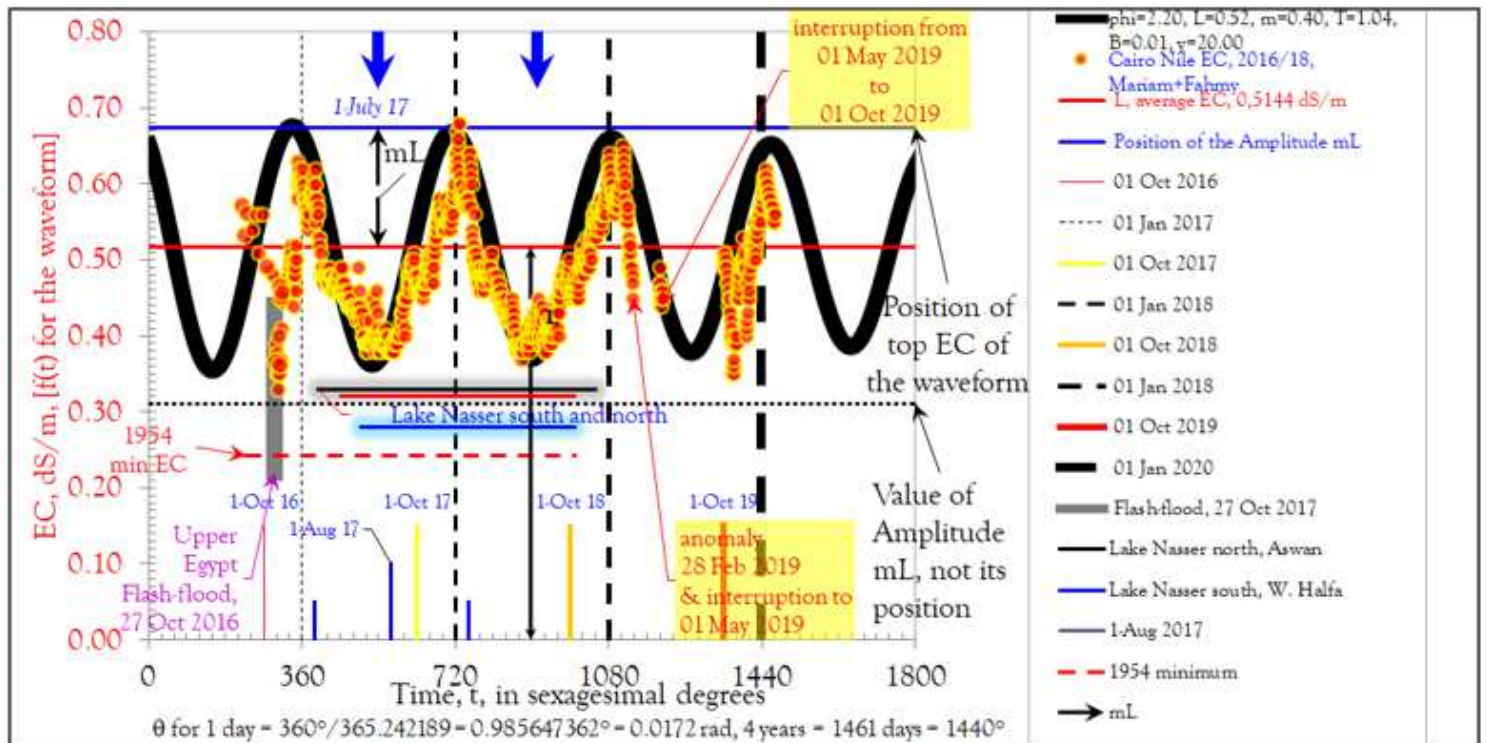


Figure 1

The waveform model fitted to the EC, dS m⁻¹, values for Cairo Nile water. The obtained waveform was to improve via introducing more measurements over four years. $f(t) = L * [1 + (m - (m \cdot \gamma / 100)) * (\sin(\gamma / (T * 0.985547362)))]$ (1.A) $f(t) = 0.5712 * [1 + (0.40 - (0.40 * 0.01/100)) * (\sin(\gamma / (1.0416 * 0.985547362)))]$... with $\gamma = 20.00$

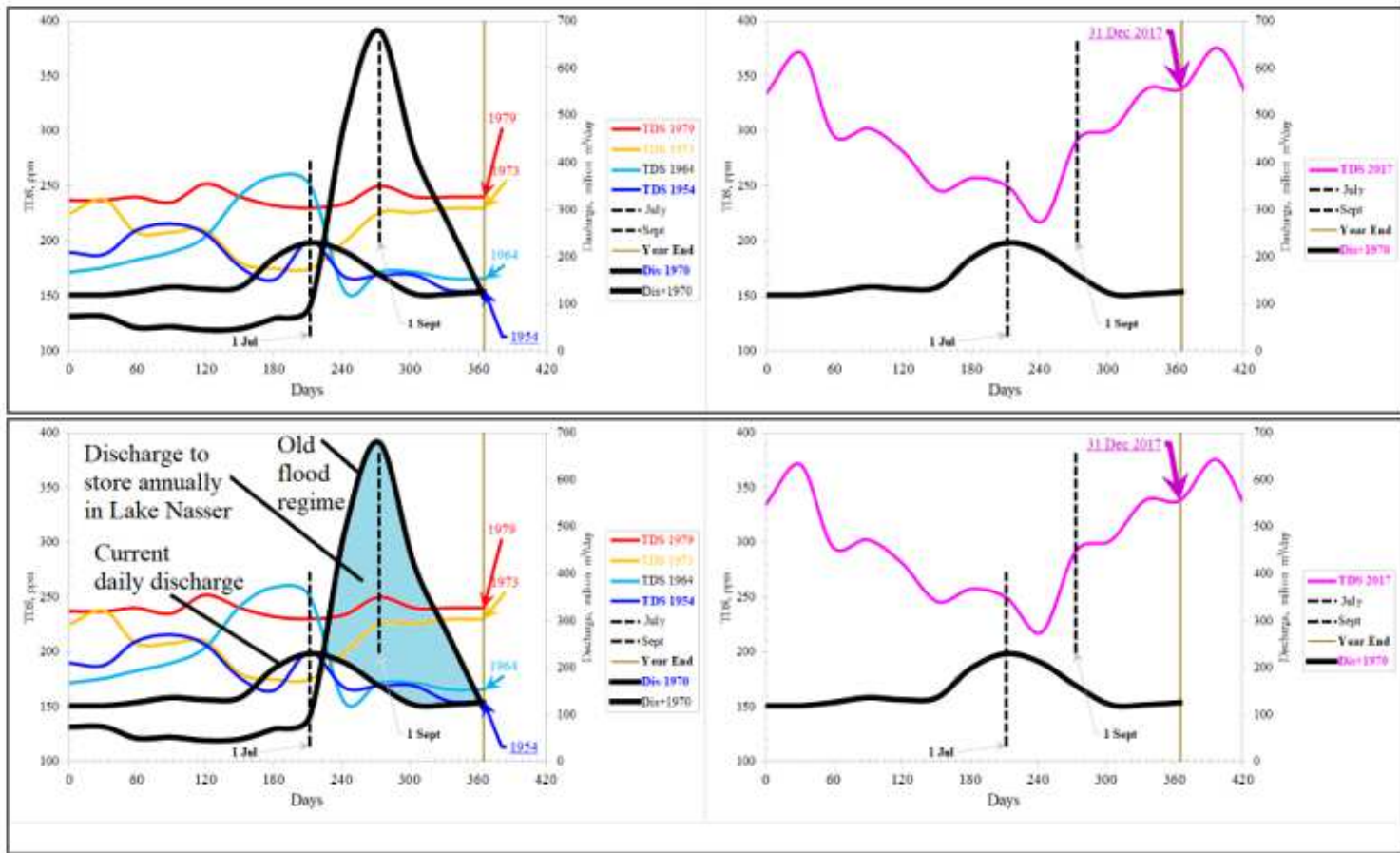


Figure 2

Diagrams showing the old (left) and the current (right) NILE discharge and TDS values at Cairo.